NOTES AND CORRESPONDENCE

Similarity Solutions for the Stratified Turbulent Rayleigh Problem[1]

GEORGE MELLOR

Princeton University, Princeton, NJ 08540

PAUL T. STRUB

Department of Atmospheric Sciences, University of California at Davis, Davis, CA 95616

21 June 1979 and 12 November 1979

ABSTRACT

The type of stratified flow suggested by the Kantha Phillips and Azad experiment is examined analytically and shown to be a self-similar, turbulent flow which includes the well-documented flat-plate, turbulent boundary-layer case. Some relevant second-moment turbulent closure model calculations are compared with the KPA data.

1. Introduction

The purpose of this note is fourfold: (i) to provide theoretical support for Wyatt's (1978b) observation that the two-layer experiment by Kantha *et al.* (1977) appears to be a self-similar problem (it is so in the ideal limit of zero curvature and infinite aspect ratio); (ii) to point out the fact that the well-established, neutral turbulent layer over a flat wall is the zero Richardson number, limiting case for these flows which one might term, *stratified, turbulent Raleigh flows*; (iii) to present model simulations for this problem which embody (i) and (ii); and (iv) to compare the model results with KPA data even though those data apparently include side wall and curvature effects (Price, 1979; Thompson, 1978; Wyatt and Kantha 1978a) which are not simulated by the model. Furthermore, the model assumes a solid wall boundary condition whereas the experiments used a porous screen.

Additionally, we have run the model including the Coriolis term and note that profiles and entrainment rates are greatly altered.

2. The basic equations

The equations and boundary conditions for a two-layered horizontally homogeneous flow are

$$\frac{\partial U}{\partial t} = \frac{\partial}{\partial z}\left(K_M \frac{\partial U}{\partial z} \right), \tag{1}$$

$$\frac{\partial \rho}{\partial t} = \frac{\partial}{\partial z}\left(K_H \frac{\partial \rho}{\partial t} \right), \tag{2}$$

$$K_M \frac{\partial U}{\partial z} \sim u_\tau^2, \quad z \to 0;$$

$$U \sim 0, \quad z \to -\infty, \tag{3a,b}$$

$$K_H \frac{\partial \rho}{\partial z} \sim 0, \quad z \to 0; \quad \rho \sim \rho_\infty, \quad z \to -\infty, \tag{4a,b}$$

where U and ρ are the mean velocity and density; u_τ is the friction velocity and ρ_∞ the constant density in the lower layer.

3. Similarity equations

We now assume

$$\frac{U}{u_\tau} = F(\eta); \quad \eta \equiv \frac{z}{\Delta(t)}, \tag{5a,b}$$

$$\frac{\rho - \rho_\infty}{\bar{\rho}(t)} = G(\eta), \tag{6}$$

where Δ and $\bar{\rho}$ are time-dependent length and density scale factors. We also assume

$$K_M = u_\tau \Delta \phi_M(\eta, \text{Ri}), \tag{7}$$

$$K_H = u_\tau \Delta \phi_H(\eta, \text{Ri}), \tag{8}$$

where

$$\text{Ri} \equiv -\frac{\dfrac{g}{\rho_0}\dfrac{\partial \rho}{\partial z}}{\left(\dfrac{\partial U}{\partial z}\right)^2} \tag{9}$$

is the local gradient Richardson number. It is believed that most closure models, some simple, some complex, reduce to (7) and (8) if the conditions for similarity exist in the form of (5a,b) and (6).

In the present development, we let u_τ = constant. However, the analysis can be easily generalized for cases where $u_\tau \propto t^n$ for arbitrary constant n.

If we now use (5a,b), (6), (7) and (8) in (1)–(4) we obtain

$$(\phi_M F')' + \frac{\Delta'}{u_\tau} \eta F' = 0, \tag{10}$$

$$(\phi_H G')' + \frac{\Delta'}{u_\tau} \eta G' - \frac{\bar{\rho}'}{\bar{\rho}} \frac{\Delta}{u_\tau} G = 0, \tag{11}$$

$$\phi_M F' \sim 1, \quad \eta \to 0; \quad F \sim 0, \quad \eta \to -\infty, \tag{12a,b}$$

$$\phi_H G' \sim 1, \quad \eta \to 0; \quad G \sim 0, \quad \eta \to -\infty, \tag{13a,b}$$

$$\text{Ri} = \text{Ri}_0 \frac{G'}{(F')^2}, \tag{14a}$$

where

$$\text{Ri}_0 \equiv - \frac{g \Delta \bar{\rho}}{\rho_0 u_\tau^2} \tag{14b}$$

is the bulk Richardson number. Primes represent differentiation with respect to η or t according to variable argument as defined in (5a,b) and (6).

Now for similarity solutions to exist, Δ'/u_τ and $\Delta\bar{\rho}'/(\bar{\rho}u_\tau)$ must be invariant. Furthermore, these parameters are not independent since, on integrating (11) from $\eta = 0$ to $-\infty$, using (13a,b), we obtain

$$\frac{\Delta'}{u_\tau} + \frac{\Delta}{u_\tau} \frac{\bar{\rho}'}{\bar{\rho}} = 0, \tag{15}$$

which integrates to $\Delta\bar{\rho}$ = constant. Therefore, the condition of similarity is that $\Delta'/u_\tau = -\Delta\bar{\rho}'/(u_\tau\bar{\rho})$ = constant. Integrating (10) from $-\infty$ to 0 we obtain

$$\Delta'/u_\tau = \left[\int_{-\infty}^0 F d\eta \right]^{-1}.$$

Following Clauser (1954), we may now define

$$\Delta \equiv \int_{-\infty}^0 \frac{U}{u_\tau} dz, \tag{16}$$

in which case

$$\int_{-\infty}^0 F d\eta = 1$$

and

$$\frac{\Delta'}{u_\tau} = 1. \tag{17}$$

We further define $\bar{\rho}$ so that

$$\int_{-\infty}^0 G d\eta = 1$$

and

$$\Delta\bar{\rho} = - \int_{-\infty}^0 (\rho - \rho_\infty) dz. \tag{18}$$

Whether or not the flow is similar, $\Delta\bar{\rho}$ is conserved and equal to $h_0 \delta\rho$ in the case where the flow is initialized with two constant density layers separated by a density jump $\delta\rho$ at $z = -h_0$. Note, then, that $\text{Ri}_0 = -g h_0 \delta\rho/(\rho_0 u_\tau^2)$.

Thus, the stratified turbulent Raleigh flow as approximated by the experiments of Kantha et al. (1977) is self-similar. This is in contrast to the Kato and Phillips (1969) experiments where it may be shown that similarity solutions do not exist; i.e., $U/u_\tau = F(\eta,t)$. However, that problem (initial $\partial\rho/\partial z$ = constant) may be rescaled so that only one parameter-free problem exists (Mellor and Durbin, 1975).

4. Law of the wall

Next to a solid wall it is known that

$$\phi_M \sim k|\eta|; \quad \eta \to 0.$$

Thus, (12a) yields

$$\frac{U}{u_\tau} \equiv F \sim \frac{1}{k} \ln|\eta| + A; \quad \eta \to 0, \tag{19}$$

where for the similar, turbulent Raleigh problem $A = A(\text{Ri}_0)$.

Eq. (19) is the inner asymptote of the outer function $F(\eta)$. On the other hand,

$$\frac{U_w - U}{u_\tau} \sim \frac{1}{k} \ln \frac{|z|}{z_0}; \quad \frac{z}{z_0} \to -\infty \tag{20}$$

is the outer asymptote of the inner law of the wall function. Here U_w is the wall velocity and z_0 the roughness height, whereas for a smooth wall $z_0 u_\tau/\nu \approx 0.14$. If we add (19) and (20), we obtain

$$\frac{U_w}{u_\tau} = \frac{1}{k} \ln \frac{z_0}{\Delta} + A. \tag{21}$$

5. The neutral turbulent Rayleigh flow

We deem it worthwhile to point out that the limiting case of zero Richardson number, of course, is the turbulent analogue of the Rayleigh problem and, as shown by Mellor and Gibson (1966), Crow (1968) and Mellor (1972), corresponds exactly to the infinite Reynolds number limit [where the operator, $U\partial(\ )/\partial x + W\partial(\ )/\partial z \to U_p \partial(\ )/\partial x$] of turbulent flat plate flow after a Gallilean transformation and differs in very small quantitative detail from well-documented flat plate data for large but finite Reynolds number. In fact, plotting flat plate data in so-called velocity defect form is supposed to remove all Reynolds number dependence.

The boundary-layer data from Klebanoff (1955) are reproduced in Fig. 1. Although, in this neutral case the mixed-layer depth is less well defined, we deduce from Klebanoff's data that the entrainment rate E based on the velocity or shear stress diminishing to 1% of its maximum value is ~ 0.25.

6. Model simulations

The model simulations include the numerical solutions of Eqs. (1), (2), (3a,b) and (4a,b) and equations for the turbulent energy and the turbulent length scale. The model further provides diagnostic equations for mixing coefficients which are dependent on the turbulent energy, length scale and velocity and buoyancy gradients. A simulation for $Ri_0 = 0$ produced the calculated results in Fig. 1, as previously described by Mellor and Yamada (1977). The most recent and directly applicable description of the model (the "level two and a half" version) has been provided by Blumberg and Mellor (1979).

In the present calculations, the molecular values of viscosity and salt diffusivity were added to K_M and K_H, respectively. The vertical and temporal resolution were sufficiently fine so that halving them again produced negligible effect. The initial conditions for the calculations were zero velocity and two constant density layers separated by a density jump $\delta\rho$ at $z = -h_0$. A surface shear stress was then impulsively applied. Initially, the flow is non-similar. A particular simulation for $Ri_0 = 100$ is represented in Figs. 2 and 3. It will be seen that similarly has very nearly been attained when $u_\tau t/h_0 \geq 50$.

Assuming that entrainment depth h corresponds to $(\rho_\infty - \rho)/\bar{\rho} \approx 0.01$, then, in Fig. 2 we obtain $h/\Delta = 0.054$ from which one can obtain the entrainment rate according to

$$E \equiv \frac{1}{u_\tau}\frac{dh}{dt} = \frac{\Delta'}{u_\tau}\frac{h}{\Delta} = \frac{h}{\Delta} . \qquad (22)$$

In Fig. 3 a detailed entrainment history, h/h_0 vs $u_\tau t/h_0$, is shown and confirms the establishment of similarity at $u_\tau t/h_0 \approx 50$.

At this point it is convenient to note that the model currently has no transition mechanism built into it so that a small initial "seeding" of K_M is prescribed near the surface. However, after $u_\tau t/h_0 \approx 20$, it is believed that the generated turbulence field is independent of the initial conditions and the subsequent development toward similarity is a valid simulation of that process.

In Fig. 4 the KPA data are plotted together with the results of model runs for a range of Ri_0 values. The data point at $Ri_0 = 0$ is very reliable since there is a great deal of data to corroborate Klebanoff's results.
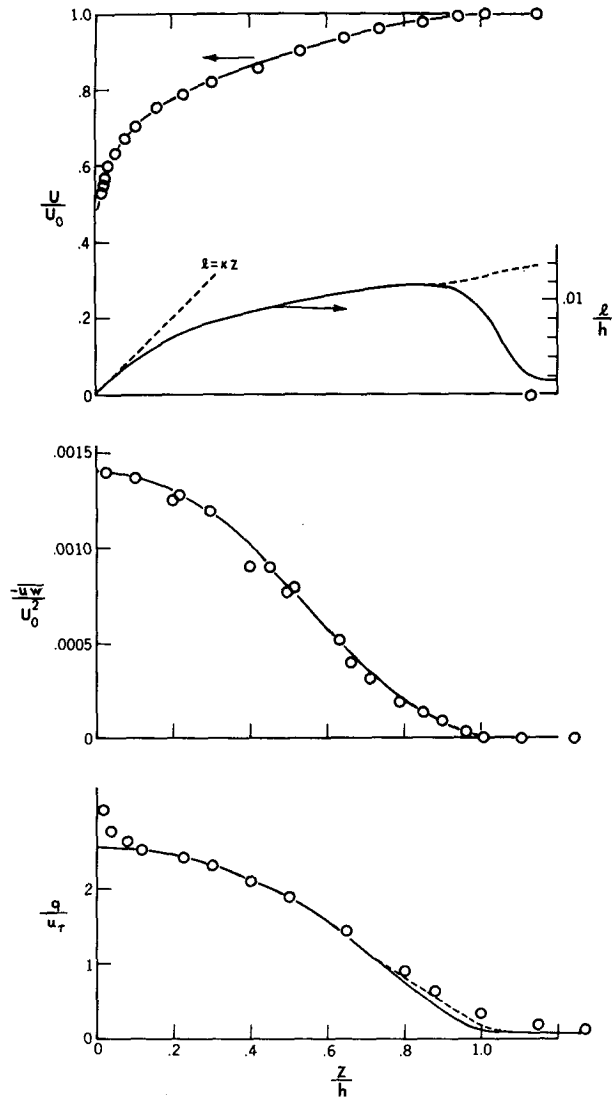

FIG. 1. Turbulent flat plate data by Klebanoff (1955). The Reynolds number is $U_0 h/\nu = 7.4 \times 10^4$; $u_\tau/U = 0.0377$ and $h/\Delta = 0.25$. The continuous curves are model results from Mellor and Yamada (1977). Two outer boundary conditions for the turbulent length scale l produce almost identical results.

The dashed line is a simple theory by Price (1979) based on a constant bulk Froude number which, by the way, provided a simple explanation for the difference in entrainment rates obtained in these experiments and in those of Kato and Phillips (1969). Price also attributes the experimental decrease in E for $Ri_0 \geq 200$ to the effects of side wall friction (see also Thompson, 1978; Wyatt and Kantha, 1978a). For $Ri_0 \leq 100$, the fact that the model predicts lower values of E than the experimental data (which, when extrapolated to $Ri_0 = 0$, would appear to be larger than the turbulent flat plate data) is not surprising in view of the additional effects of curvature
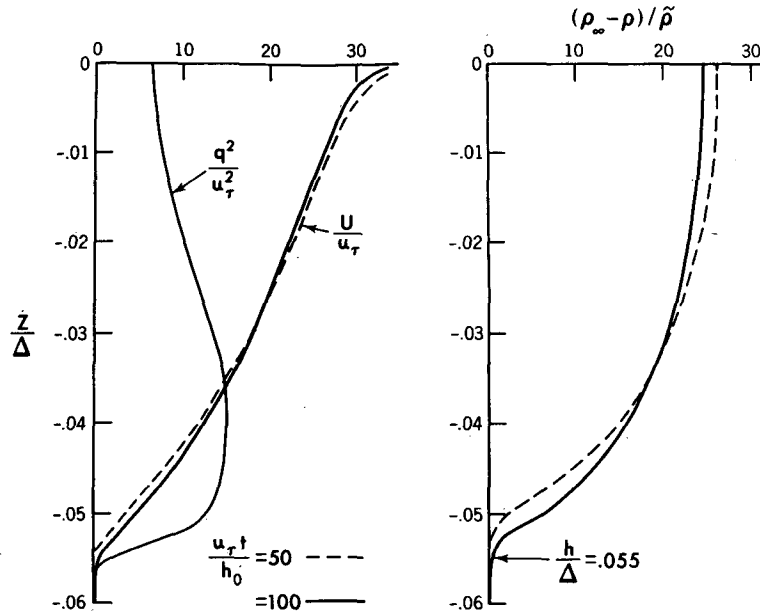
FIG. 2. Model profiles of mean velocity, (twice the) kinetic energy and density in similarity form for $Ri_0 = 100$.

and wall porosity (Wyatt and Kantha, 1978a) which are not simulated by the model.

Now, according to (21), the wall or, in the KPA case, the screen velocity will decrease as Δ increases for constant u_τ and z_0. This is in accordance with observation as reported by KPA. The predicted rate of decrease is ~40% too low but this discrepancy is reduced to about 20% if the computed, non-similar behavior (for small time) is used in conjunction with (20). However, in view of the dissimilarities

in the model and experimental flows, particularly near the screen, agreement or disagreement may be coincidental.

We note finally that the shape of the density profiles are quite similar to those sketched by Wyatt (1978b) for conductivity probe traverses taken in the same tank and under the same conditions as the KPA experiments [see, also, Kantha (1978) for additional density profile data]. From these observations, she anticipated that the flow appeared to be self similar.
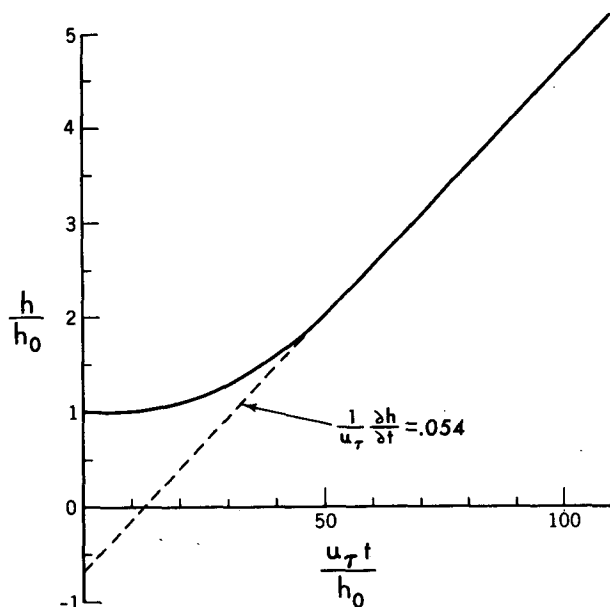
7. Effect of the Coriolis parameter

Wyatt also drew attention to the fact that the laboratory density profiles are dissimilar to field observations in that the latter, generally, are nearly constant in the surface layer and then change rather abruptly at the interface. To explore the simplest cause of these differences we have inserted the Coriolis term in the equations of motion which, in place of (1), becomes

$$\frac{\partial \bar{U}}{\partial t} + if\bar{U} = \frac{\partial}{\partial z}\left(K_M \frac{\partial \bar{U}}{\partial z}\right), \qquad (23)$$

where we use the complex velocity, $\bar{U} = U + iV$. Our first calculation with an f, chosen rather arbitrarily, resulted in $fh_0/u_\tau = 0.37$. The near steady state[2] results for $Ri_0 = 100$ and when

FIG. 3. Calculated variation in mixed layer depth versus time for $Ri_0 = 100$.

[2] If one starts up the calculation with an impulsive wind stress, inertial oscillations result and persist indefinitely (Mellor and Durbin, 1975). Alternately, double the initial wind stress at $t = \pi/f$ and the flow approaches near steady state. The later strategy was used for the calculations of Fig. 5.
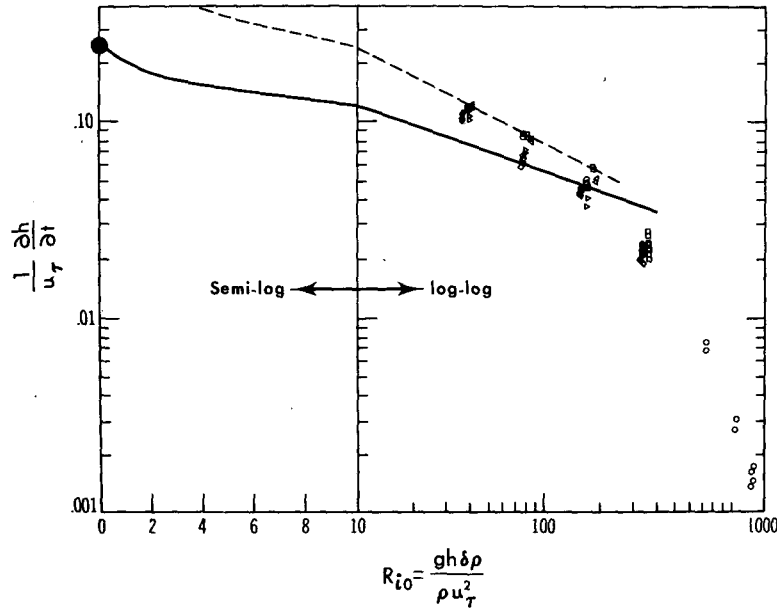
FIG. 4. The entrainment data of Kantha, Phillips and Azad (1977). The large circular data point at $Ri_0 = 0$ is the turbulent flat plate value of entrainment. The dashed line is the $Ri_0^{-1/2}$ theory of Price (1979) when side-wall friction is neglected. The solid line results from model calculations.

$u_\tau t/h_0 = 100$ are shown in Fig. 5 as solid lines. For comparison a neutral case, $Ri_0 = 0$, is shown as dashed lines in Fig. 5.

It may be remarked that, using a prognostic, turbulent length scale equation (with constants determined from channel flow and boundary-layer flow), we now obtain thicker, neutral Ekman layers than when we used a diagnostic, algebraic, length-scale equation with a constant determined by guessing at a neutral Ekman layer height ($\sim 0.3 u_\tau/f$).

We believe that available evidence suggests that the new result is to be preferred, but neutral or near-neutral profile data as summarized by Caldwell et al. (1972) and McPhee and Smith (1976) are not conclusive. In fact, many of the profiles do not satisfy a property of (23) that the integrals of U/u_τ and V/u_τ with respect zf/u_τ be zero and unity, respectively.

The addition of the Coriolis parameter for the two-layer, stratified case greatly reduces the entrain-
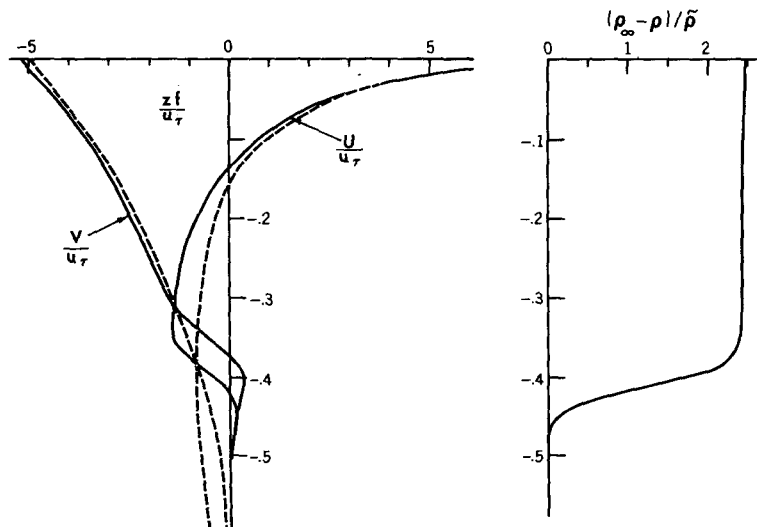

FIG. 5. Mean velocity and density profiles with addition of the Coriolis term to the momentum equation. The solid lines correspond to $fh_0/u_\tau = 0.37$, $Ri_0 = 100$; we obtain $E \approx 0.01$. The dashed lines are the stationary, neutral Ekman layer.

ment rate from $E = 0.054$ to $E \approx 0.01$, the latter being a rough estimate since the flow is no longer similar, E is not constant in time and (22) no longer applies. The decrease in E, of course, is due to the fact that the stress divergence is nearly balanced by the Coriolis acceleration term in (23).

Finally, it seems safe to conclude that the difference in density profiles for $f = 0$ and $f \neq 0$ illustrated in Figs. 2 and 5 is primarily and simply related to the resulting decrease in E in the latter case, thereby allowing the mixed layer to mix more thoroughly.

REFERENCES

Blumberg, A. F., and G. L. Mellor, 1979: A coastal ocean numerical model. *Proceeding of the Symposium on the Mathematical Modelling of Estuarine Physics*, Springer-Verlag (in press).

Caldwell, D. R., C. W. Van Atta and K. N. Helland, 1972: A laboratory study of the turbulent Ekman layer. *Geophys. Fluid Dyn.*, **3**, 125–160.

Clauser, F., 1954: Turbulent boundary layers in adverse pressure gradients. *J. Aero. Sci.*, **21**, 91–108.

Crow, S., 1968: Turbulent Rayleigh shear flow. *J. Fluid Mech.*, **32**, 113–130.

Kantha, L. H., 1978: On surface-stress-induced entrainment at a buoyancy interface. Rep. TR78-1, Dept. of Earth and Planetary Sci., The Johns Hopkins University.

——, O. M. Phillips and R. S. Azad, 1977: On the turbulent entrainment at a stable density interface. *J. Fluid Mech.*, **79**, 753–758.

Kato, H., and O. M. Phillips, 1969: On the penetration of a turbulent layer into stratified fluid. *J. Fluid Mech.*, **37**, 643–655.

Klebanoff, P. S., 1955: Characteristics of turbulence in a boundary layer with zero pressure gradient. NACA Rep. 1247.

McPhee, M. G., and J. D. Smith, 1976: Measurements of the turbulent boundary layer under pack ice. *J. Phys. Oceanogr.*, **5**, 696–711.

Mellor, G. L., 1972: The large Reynolds number asymptotic theory of turbulent boundary layers. *Ind. J. Eng. Sci.*, **10**, 851–873.

——, and D. M. Gibson, 1966: Equilibrium turbulent boundary layers. *J. Fluid Mech.*, **24**, 225–253.

——, and P. A. Durbin, 1975: The structure and dynamics of the ocean mixed layer. *J. Phys. Oceanogr.*, **5**, 718–728.

——, and T. Yamada, 1977: A turbulence model applied to geophysical fluid problems. *Proceedings: Symposium on Turbulent Shear Flows*, Pennsylvania State University, 1–14.

Price, J. F., 1979: On the scaling of stress-driven entrainment experiments. *J. Fluid Mech.*, **90**, 509–529.

Thompson, R. O. R. Y., 1978: Application of Kato, Kantha and Phillips experiments to the ocean. *Ocean Modelling*, No. 10, 4–6.

Wyatt, L. R., and L. Kantha, 1978a: Further discussion on interpreting laboratory models of the mixed layer. *Ocean Modelling*, No. 13, 5–6.

——, 1978b: Mixed layer development in an annulus tank. *Ocean Modelling*, No. 17, 6–8.